Chemistry–A European Journal
Research Article
doi.org/10.1002/chem.202403939
Chemistry Europe
European Chemical Societies Publishing
www.chemeurj.org

Proximity Effects and Aggregation of Hamilton-Receptor Barbiturate Host–Guest Complexes Probed by Cross-Metathesis and ESI MS Analysis

Chenming Li,[a] Pascal Mai,[a] Niclas Festag,[a] Anja Marinow,[a] and Wolfgang H. Binder*[a]

The molecular environment around supramolecular bonding systems significantly affects their stability and the assembly of host–guest complexes, most prominent for hydrogen bonds (H-bonds). Hamilton receptor-barbiturate host–guest complexes are well-known in solution, typically forming a 1:1 molar ratio complex. However, within a polymer matrix, these complexes can form higher-order assemblies, deviating from the standard 1:1 complex, which are challenging to characterize and often require lab-intensive methods. In this study, a novel Hamilton receptor (**H**) was equipped with cyclopentene moieties and used as a host to form host–guest complexes (**H**–**B**) with allobarbital (**B**), followed by covalent crosslinking. UV-Vis spectroscopy titration experiments in different solvents and at various temperatures revealed that polar solvents containing additional H-bonding sites significantly reduce the formation of the 1:1 **H**–**B** complex, as indicated by a reduced association constant. Higher-order aggregates (**HH**-dimer, **HHH**-trimer) were subsequently detected via an alkene cross-metathesis (**CM**) reaction to fix the assemblies covalently, followed by analysis via electrospray ionization mass spectrometry (ESI MS). This two-step method, firstly via **CM** fixation followed by ESI MS, was extended to study the **H**–**B** model complex within a polyisobutylene (**PIB**) matrix, presenting a direct method to analyze the complex host–guest assembly in solvent-free (polymer) environments.

Introduction

Supramolecular structures, such as hydrogen bonding (H-bonding) systems, constitute highly relevant structural units of molecular self-assembly, bridging biological and synthetic sciences by implementing dynamic properties into materials and molecules. Similar to their behavior in solution, supramolecular bonds[1] in polymers also exhibit (partially) reversible formation and reformation via host–guest complexes, depending on their bonding strength, their exchange kinetics, as well as influences from the surrounding micro- and nano-environment. Phase segregation, crystallization, or the assembly of polymers is an additional structural principle where often limited diffusion is coupled to an anisotropic environment, with only rudimentary knowledge about the formation of host–guest complexes therein as both diffusion and spatial in-homogeneities, as well as anisotropy, prevail.[2] Therefore, when embedded into polymers, many host–guest complexes display an essentially modified exchange behavior compared to their solution counterparts,[1b,c] often characterized by clustering and aggregation effects forming host–guest complexes different from the expected 1:1 stoichiometry.[3] Thus, for example, the effective strength of H-bonds is influenced by a subtle interplay between their intrinsic chemical structure (e.g., by substituent effects[4]), the surrounding polarity of the medium, their concentration as well as the microenvironment locally surrounding the H-bonds.[1c] Clusters of H-bonds are often formed in solid polymers, contributing most importantly to macroscopic effects, such as self-healing and reformation of the initial structures,[1c,3b,5] resulting in enormously different melt-flow behavior of the materials by their now changed relaxation behavior.[6] Whereas in most cases the same H-bonds, when affixed to larger groups such as polymer chains, do not differ in strength compared to the unsubstituted H-bond in well-solvating solvents,[7] a significant effect on the formation of different host–guest complexes observed from the local micro-environment on the associating H-bonds in case of attached polymers with reduced solubility.

We and others in the past have investigated the competing phase segregation effects in supramolecular polymers bearing H-bonds in both solutions and the solid state, wherein the molecular recognition elements are based on multiple H-bonding moieties (see Figure 1a), such as the thymine-diaminopyridine (THY-DAP), the thymine-diaminotriazine (THY-DAT), the ureidopyrimidinone dimers (UPy-UPy), and Hamilton-receptor-barbiturate (HW–Ba) host–guest complexes.[1b,c,3,8] By tuning the segregation between the polymer chains, H-bonded supramolecular dendrons can be formed, displaying a complex assembly behavior into nanophases or the formation of (chain-extended) pseudo-block copolymers.[9] While attractive H-bond-

[a] C. Li, P. Mai, N. Festag, A. Marinow, W. H. Binder
Faculty of Natural Science II, Institute of Chemistry, Macromolecular Chemistry, Martin Luther University Halle-Wittenberg, von-Danckelmann-Platz 4, Halle/Saale D-06120, Germany
E-mail: wolfgang.binder@chemie.uni-halle.de

Supporting information for this article is available on the WWW under https://doi.org/10.1002/chem.202403939

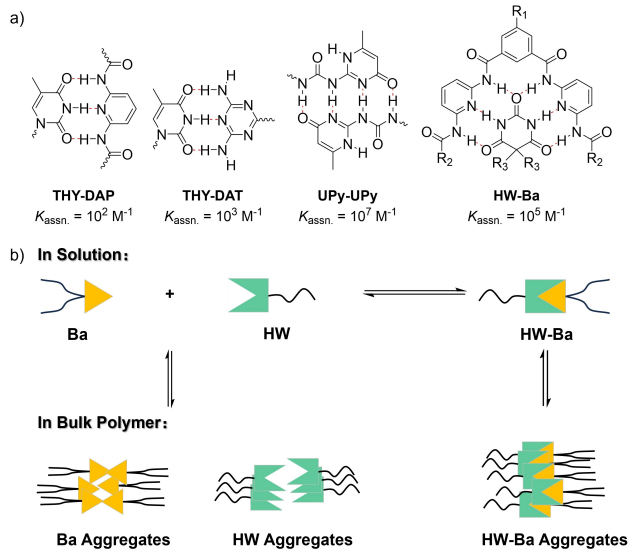

Figure 1. a) The molecular recognition elements of thymine-diaminopyridine (THY-DAP), thymine-diaminotriazine (THY-DAT), ureidopyrimidinone dimer (UPy-UPy), and Hamilton receptor-barbiturate (HW–Ba) host–guest complexes based on multiple H-bonds (values of the association constants $K_{assn.}$s were taken from ref. [14]); b) possible association between HW and Ba in solution and bulk polymer forming aggregates and the backbone segregation during the assembly process.

ing in solution usually exceeds phase segregation effects between the polymer chains, the situation is different in polymers devoid of solvent, either in the melt state, the (semi−)crystalline or liquid crystalline state,[10] as now segregation can become dominant over the attractive H-bonding, also leading to clustering effects not observed in solution (see Figure 1b). Methods to study dynamics and thermodynamics of bond-breaking/reformation are currently only indirect ones, mainly using melt rheology[11] or magic-angle spinning (MAS) NMR spectroscopy[1b,12] with cluster sizes estimated by X-ray techniques.[1b,6c,11a,h,13]

Multiple H-bonding systems, such as the UPy-UPy or the HW–Ba, have become crucial for generating stable and reversible bonds in bulk-polymers. The HW–Ba host–guest complexes herein have been intensely studied in solutions, displaying a strong and specific assembly with an association constant $K_{assn.}$ up to 10^6 M^{-1}[15] and a directional nature owing to the stereo-specified sextuple H-bonds, resulting in distinct 1:1 complexes in solution. Various chemical modifications have been accomplished to tune the assembly behavior of the HW receptor by modifying substituents at the outer rim[13f,16] or forming cyclic HW receptors.[16c,17] These modifications open the possibility of embedding further functionalities for a subsequent covalent modification to study the assembly processes between the HW–Ba system, as well as further by a covalent fixation after H-bonding formation, a strategy similar to the concept of Scherman and Meijer.[18] Herein, a cross-metathesis (**CM**) chemistry of adjacent ene-functionalities linked to the HW and Ba molecules was used to fix the specific H-bonded assembly of the HW–Ba host–guest complexes. We here present a method to investigate H-bond clustering effects in solutions and bulk-polymers using covalent **CM** chemsitry to tether transient or thermodynamically stable structures. This approach provides direct information that often is not accessible through spectroscopic methods. Our approach (see Figure 2) is based on a combination of supramolecular assembly via sextuple H-bonds between a novel Hamilton receptor (**H**) bearing cyclopentene moieties at the outer rim, and allobarbital (**B**) with allyl groups, followed by **CM** reactions to fix the formed assemblies covalently, which were subsequently analyzed by electrospray ionization mass spectrometry (ESI MS). We conducted this two-step covalent-fixation-ESI-analysis in different solvents at various concentrations of the **H**–**B** supramolecular binding partners as a proof-of-principle study, followed by a preliminary investigation inside a solvent-free polyisobutylene (**PIB**) matrix, finally aiming to understand the behavior of such supramolecular bonds in nonsolvating polymeric environments.

Results and Discussion

Model Hamilton Receptor-Barbiturate (H–B) Host–Guest Chemistry in Solution

Since the first reports on synthesizing the Hamilton receptor for barbiturates in the 1980s to 1990s,[15,19] variations of such receptors have been generated with multifold structures and functionalities.[13f,16b,d,17d,20] We herein designed a novel Hamilton receptor **H** bearing cyclopentene moieties at its outer rim (Figure 2), able to undergo a subsequent **CM** reaction with Grubbs catalysts. The cyclopentene moieties at the outer rim of the Hamilton receptor were expected to change the specific formation of the desired host–guest complex with barbiturates only slightly, analogous to other modifications of the Hamilton receptors reported previously.[17d,20b,e,21] Similarly, the bis-allyl-barbital **B** has been equipped with **CM**-reactive allyl groups on the C5 position, prepared as described in the supporting information (for the detailed synthesis, see *Supporting Informa-*

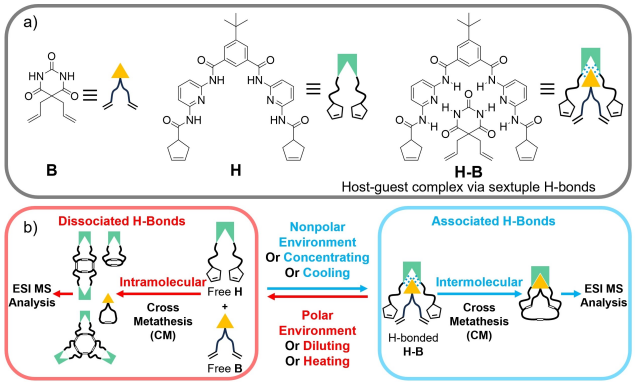

Figure 2. a) Chemical structures and schematic illustration of the model Hamilton receptor **H** and barbiturate **B** and their host–guest complex via sextuple H-bonds; b) the concept of this work: upon concentrating, cooling, or in a nonpolar environment, **H** and **B** associate to form a specific **H**–**B** assembly and higher-order assemblies (=aggregates); upon diluting, heating, or in a polar environment, **H** and **B** dissociate and cross-metathesis (**CM**) can be used to fix host/guest assemblies for subsequent ESI MS analysis.

tion, SI 1.3). Conceptually, the 1 : 1 **H**–**B** host–guest complex can be fixed covalently after its formation. However, it also allows the detection of other formed complexes of different stoichiometry by ESI MS measurements to reveal their chemical nature and relative amounts. In bulk polymers, then devoid of solvents, we previously observed the formation of host–guest complexes different from the 1 : 1 stoichiometry in solution induced by phase segregation effects from the polymer chains.[1b,3b,13d,22] Here, the approach using covalent crosslinking via **CM** after forming the host–guest complexes presents a first step to reveal such host–guest structures inside the solvent-free environment.

To explore the influence (solvents, temperature) on the formation of the host–guest complexes of the modified **H** with **B**, the association constant $K_{assn.}$ of the **H**–**B** complex was determined in various solvents. As reported previously,[24] titration, in-situe followed by UV-Vis spectroscopy was employed due to its fast and sensitive determination and the low demand on the amount of the substrates. As depicted in Figure 3a), data collected from the UV titration were mathematically fitted to generate such a curve to obtain the $K_{assn.}$ under different conditions using the online program BindFit (available via http://supramolecular.org;[24,25] for UV titration, fitting, and method details, see *Supporting Information*, SI 2). All the determined $K_{assn.}$s are listed in Table 1. In Figure 3b), the association constants $K_{assn.}$s of **H** with **B** in various solvents are plotted against their dielectric constants,[23] indicative of the effects of solvent polarity on the stability of the **H**–**B** complex. As expected, in toluene (Tol) the **H**–**B** host–guest complex displays the highest stability with $K_{assn.}$ equal to ~10^5 M^{-1}, while in the halogenated solvents such as chloroform ($CHCl_3$) and dichloromethane (DCM), $K_{assn.}$ is reduced by an order of magnitude to ~10^4 M^{-1}. In 1,2-dichloroethane (DCE), the **H**–**B** association is further weakened to $K_{assn.}$~10^3 M^{-1}. Interestingly, in α,α,α-trifluorotoluene (TFT), a solvent comparable to Tol but with an enhanced polarity and distinct fluorophilicity, the **H**–**B** complex displays a surprising stability (see Entry S15 in Table 1), aligning with previously reported solvophobic interactions[26] that can enhance the H-bond strength. As expected, all other polar solvents (such as 1,4-dioxane, hexafluoro-2-propanol, isopropanol, acetonitrile, and THF, see Entry S4–S13) strongly reduce the stability of the host–guest complex, with association constants $K_{assn.}$s in the range of ~10^2 M^{-1}. To further examine that the addition of extra donors/acceptors, besides polarity, leads to the reduction of H-bond strength, $K_{assn.}$ of the **H**–**B** complex was determined in toluene-methanol mixtures with increasing content of MeOH in Tol to detect the critical concentration of MeOH required to reduce the stability of the

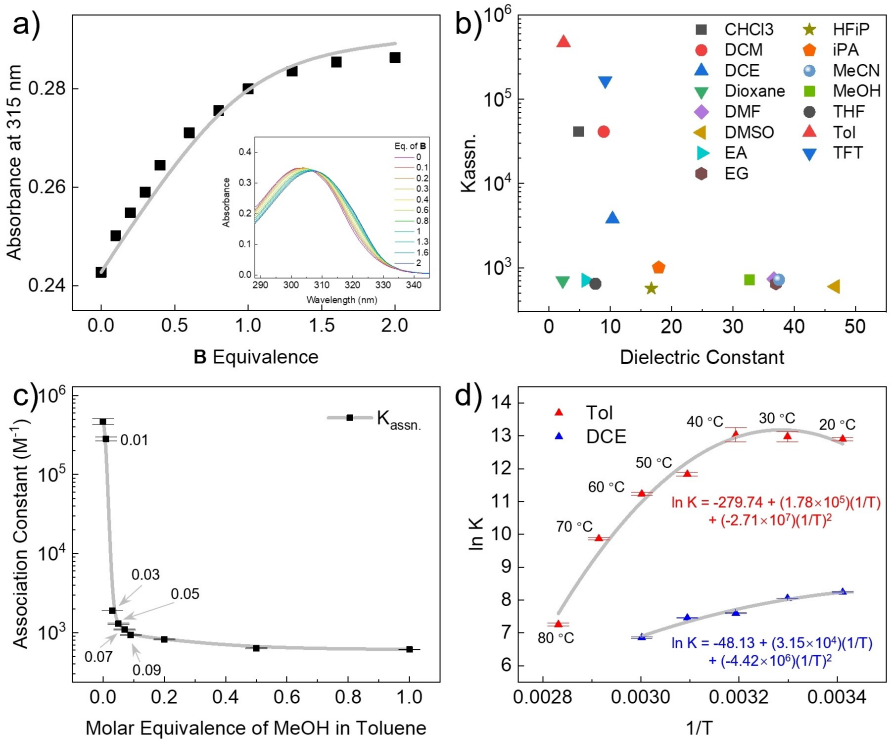

Figure 3. a) Data fitting from UV-Vis spectroscopy titration to determine the association constant $K_{assn.}$ (figure-insert shows the UV-Vis spectrum at different [**H**]:[**B**] ratios); association constants K_{assn}s of the **H**–**B** model host–guest complex in various solvents at 20 °C plotted against their dielectric constants taken from the literature [23]; the detailed $K_{assn.}$s are listed in Table 1 (each determination was repeated 3–5 times to ensure reproducibility; for titration, fitting, and method details, see *Supporting Information*, SI 2); c) association constants of the **H**–**B** model in toluene + methanol mixtures (the line is a guide for the eye only; error bars are based on fitting errors); d) van't Hoff plot of association constants of the model compounds in toluene (Tol) and 1,2-dichloroethane (DCE) at various temperatures (grey curves and equations are from the fitting of data using a polynomial function; error bars are based on fitting errors; for fitting details, see *Supporting Information*, SI 2.2).

Table 1. Dielectric constants of solvents and association constants $K_{assn.}$ and the Gibbs-energy (ΔG) of the **H**–**B** model host–guest complex in various solvents.

Entry	Solvent	Abbreviation	Dielectric Constant [a]	$K_{assn.}$ /M^{-1} [b]	ΔG/kJ mol^{-1} [c]
S1	Chloroform	$CHCl_3$	4.8	4.13×10^4	−25.9
S2	Dichloromethane	DCM	8.9	4.12×10^4	−25.9
S3	1,2-Dichloroethane	DCE	10.4	3.78×10^3	−20.1
S4	1,4-Dioxane	Dioxane	2.2	7.02×10^2	−16.0
S5	N,N-Dimethylformamide	DMF	36.7	7.34×10^2	−16.1
S6	Dimethyl Sulfoxide	DMSO	46.7	5.96×10^2	−15.6
S7	Ethyl Acetate	EA	6.0	7.08×10^2	−16.0
S8	Ethylene Glycol	EG	37.0	6.46×10^2	−15.8
S9	Hexafluoro-2-propanol	HFiP	16.7	5.66×10^2	−15.4
S10	2-Propanol	iPA	17.9	9.99×10^2	−16.8
S11	Acetonitrile	MeCN	37.5	7.18×10^2	−16.0
S12	Methanol	MeOH	32.7	7.12×10^2	−16.0
S13	Tetrahydrofuran	THF	7.6	6.44×10^2	−15.8
S14	Toluene	Tol	2.4	4.69×10^5	−31.8
S15	α,α,α-Trifluorotoluene	TFT	9.2	1.67×10^5	−29.3

* [a] The dielectric constants were taken from the ref. [23]; [b] determined by UV-Vis spectroscopy titration at 20 °C (each determination was repeated 3–5 times to ensure reproducibility; for details, see *Supporting Information*, SI 2); [c] calculated by $\Delta G = RT \ln K_{assn}$.

host–guest complex. As demonstrated in Figure 3c), as the MeOH content increases up to a molar ratio of MeOH/Tol = 0.03 (MeOH = 0.03, Tol = 1), the stability indicated by $K_{assn.}$ is reduced significantly by two orders of magnitude. A further increase of the MeOH content to 0.2 equivalents further reduces the stability ($K_{assn.}$ to ~10^2 M^{-1}) comparable to that in other polar or H-bonding-replacing solvents, such as HFiP, EA, and DMSO. This extreme reduction in $K_{assn.}$ upon the addition of MeOH to Tol demonstrates that even a subtle change in the micromolecular environment, from a purely nonpolar aprotic medium to a slightly polar protic medium, can result in a significant weakening of the H-bonds in the **H**–**B** model host–guest complex.

To probe the impact of the micro-environment on the thermodynamics of the **H**–**B** host–guest complex, van't Hoff plots were employed as outlined in Figure 3d) in two different solvents (Tol, DCE) via temperature-dependent measurements. Similar to previously reported studies utilizing van't Hoff plot to analyze the thermodynamics of supramolecular systems,[27] including HW–Ba complexes,[28] the $K_{assn.}$ of the **H**–**B** model host–guest complex obtained from UV titrations at various temperatures was fitted using a second-order polynomial function. This approach accounts for the nonlinearity arising from the non-constant standard enthalpy change over the selected temperature range (for fitting details, see *Supporting Information*, SI 2.2).[29] At temperatures of 20–40 °C the **H**–**B** model complex remains stable with $K_{assn.}$ unchanged but starts to decline at temperatures above 40 °C, while in DCE, $K_{assn.}$ is steadily reduced as temperature increases, starting from 20 °C and thereon, indicating different contributions from enthalpic and entropic factors. Indeed, known from the enthalpy change ΔH and the entropy change ΔS (see Table 2) obtained from the fitting, at a temperature below 40 °C, the association of the **H**–**B** model complex in Tol is largely entropy-driven, while that in DCE is a largely enthalpy-driven process over the whole temperature range (20–60 °C). Additionally, as temperature increases, the absolute value of the Gibbs energy change ΔG determined in Tol decreases, indicative of a reduced association between the model **H** and **B**. However, the temperature effect in DCE is less significant, evidenced by the barely changed ΔG over the whole temperature range. Therefore, the molecular surroundings indeed affect the thermodynamics of the **H**–**B** model complex by altering the contribution of the enthalpy and the entropy of the H-bonding process.

Probing Covalent Fixation of the H–B Host–Guest Complexes via Cross-Metathesis (CM) Chemistry

Several reactions were carried out to covalently fix the **H**–**B** model host–guest complexes with a 1:1 stoichiometry [**H**]:[**B**] and aggregates with different stoichiometries (e.g., dimer **cm-HH**, trimer **cm-HHH**, and others as indicated) under various conditions (see Table 3) using cross-metathesis (**CM**) reaction. As illustrated in Figure 4a), the **H** and **B** model compounds, the Grubbs catalyst (10 %mol), and the degassed solvent were placed in a vial in a glovebox with an N_2 atmosphere. The vial was heated for 24 hours before ^{1}H NMR spectroscopy was used to prove the conversion by monitoring the resonances of the initial alkenes at δ = 5.62, 5.36, 4.95, and 4.82 ppm vs. the newly formed alkenes at δ = 5.57, 5.25, and 5.19 ppm. Details of the reaction, the conversion, the catalysts, and the concentrations used are shown in Table 3. For Entry 1, the reaction was carried out at 100 °C in Tol with 0.01 M as the concentration of **H** or **B** in a ratio of 1:1. Grubbs catalyst 3rd generation (G3) was chosen

Table 2. Enthalpy ΔH, entropy ΔS, and the Gibbs energy ΔG of the **H**–**B** model host–guest complex in toluene (Tol) and 1,2-dichloroethane (DCE) at various temperatures.

		In Toluene (Tol)			In 1,2-Dichloroethane (DCE)		
T /°C	T /K	ΔH/kJ mol^{-1}	ΔS /kJ mol^{-1} K^{-1}	ΔG /kJ mol^{-1}	ΔH /kJ mol^{-1}	ΔS /kJ mol^{-1} K^{-1}	ΔG /kJ mol^{-1}
20	293	58.06	0.30	−29.47	−11.88	0.03	−20.06
30	303	7.30	0.13	−31.59	−20.16	0.00	−20.20
40	313	−40.22	−0.03	−32.09	−27.91	−0.03	−20.07
50	323	−84.79	−0.17	−31.12	−35.18	−0.05	−19.70
60	333	−126.68	−0.29	−28.81	−42.01	−0.07	−19.12
70	343	−166.13	−0.41	−25.28	–	–	–
80	353	−203.35	−0.52	−20.63	–	–	–

* The enthalpy ΔH, the entropy ΔS, and the Gibbs energy ΔG of the **H**–**B** model host–guest complex were calculated from the constants obtained from the fitting of the Figure 3d); for fitting details, *Supporting Information*, SI 2.2.

Table 3. Reaction conditions for the cross-metathesis (**CM**) reaction to fix the **H**–**B** model complex and their possible aggregates, and the conversion calculated by ^{1}H NMR spectra.

Entry	T/ °C	Solvent	Concentration/ M [a]	Catalyst [b]	Conversion [c]
1	100	Tol-d_8	0.01	G3	100%.
2	50	Tol-d_8	0.01	G3	89.4%
3	50	DCE	0.1	G3	89.5%
4	50	MeOD	0.01	G3	78.8%
5	50	DCE	0.1	G2	97.6%
6	50	PIB [d]	–	G3	97.3%

* [a] Concentration refers to **H** or **B** in a 1:1 ratio; [b] G3: Grubbs catalyst 3rd generation; G2: Grubbs catalyst 2nd generation; catalyst load was kept at 10% mol for all entries; all reactions were carried out in a glovebox under an N_2 atmosphere; [c] the conversion was calculated by the ratio of the integral of unreacted alkene and the product ene; for detailed calculations and NMR spectra for all entries, see *Supporting Information*, SI 3; [d] **PIB** was used as the reaction matrix; for detailed experimental conditions and process, see *Supporting Information*, SI 1.3.

due to its known fast initiation for **CM** reactions, allowing an efficient fixation of the **H**–**B** model complex and its potential aggregates. As shown in Figure 4b), a complete conversion of model compounds could be observed as evidenced by the shifted ^{1}H resonances of the alkenes (from $\delta = 5.62$ in the black spectrum to $\delta = 5.57$ ppm in the red spectrum) and the disappearance of the alkene protons ($\delta = 5.36$, 4.95, and 4.82 in the red spectrum) and the newly formed alkene peak at $\delta =$ 5.58 ppm as compared to the control NMR spectrum in black. At a reaction temperature of 100 °C, the stability of the H-bonds is strongly reduced, as is consequently the formation of the **H**–**B** host–guest complex. Therefore, a reaction at 50 °C with other conditions was carried out, as shown in Entry 2. In Figure 4b), the NMR spectrum (shown in blue) shows a conversion of 89.4%, as demonstrated by the residual alkene protons from **B**. Owing to the limited solubility of the components at 50 °C, DCE was used as a non-H-bond-replacing solvent to offer a higher concentration of the **H** and **B** (Entry 3), expected to lead to higher stabilities of the host–guest complex **H**–**B**. We also conducted a trial in MeOH (Entry 4), anticipated to reduce the formation of specific **H**–**B** host–guest complexes. Furthermore, Grubbs catalyst 2nd generation (G2) was also tested (Entry 5), which showed a slightly higher conversion at 50 °C. We further conducted the **CM** reaction of the **H** and **B** model compounds directly inside a bulk polyisobutylene (**PIB**) devoid of solvent to probe the formation of aggregates inside a solvent-free environment (Entry 6). In this reaction (see the experimental setup in Figure 7), the **H** and **B** model compounds were mixed with the Grubbs catalyst and the **PIB** polymer at room temperature using THF to reach homogeneity, followed by a quick evaporation of THF at room temperature in vacuum to avoid **CM** in the solution state. Subsequently, the reaction was heated at 50 °C in a glovebox under an N_2 atmosphere for 24 hours, and the conversion of this reaction (see Table 3, Entry 6) demonstrates a successful **CM** reaction inside the **PIB**. Overall, the data indicate that a successful **CM** reaction can be employed, both in solution and the solid state, to generate a conversion of **CM** ranging from 78–100%, using either G3 or G2 catalysts at temperatures (50 °C) where the **H**–**B** host–guest complexes are expected to be formed, together with potential formation of other aggregates.

ESI MS Analysis of the Covalently Fixed Complexes from Cross-Metathesis (CM) Reactions

Subsequently, the reaction mixtures were analyzed using ESI MS to identify the products formed via the **CM** reaction. Potentially, these products can consist of a) the cyclic reactants (**cm-H** or **cm-B**) resulting from intramolecular **CM** reactions (macrocyclization of individual **H** or **B** model compounds); and b) from 1:1 host–guest complexes (**cm-HB**) or from other aggregates formed via H-bonds and fixed through intermolecular **CM** reactions (examples are **cm-HH**, **cm-HHH**). The analysis by ESI MS was conducted firstly qualitatively to identify specific forms. Using Entry 1 as an example, as shown in Figure 5a), the products via the intramolecular **CM** were found as cyclized **cm-B** and **cm-H**, resulting from the ring-closing of the allyl/

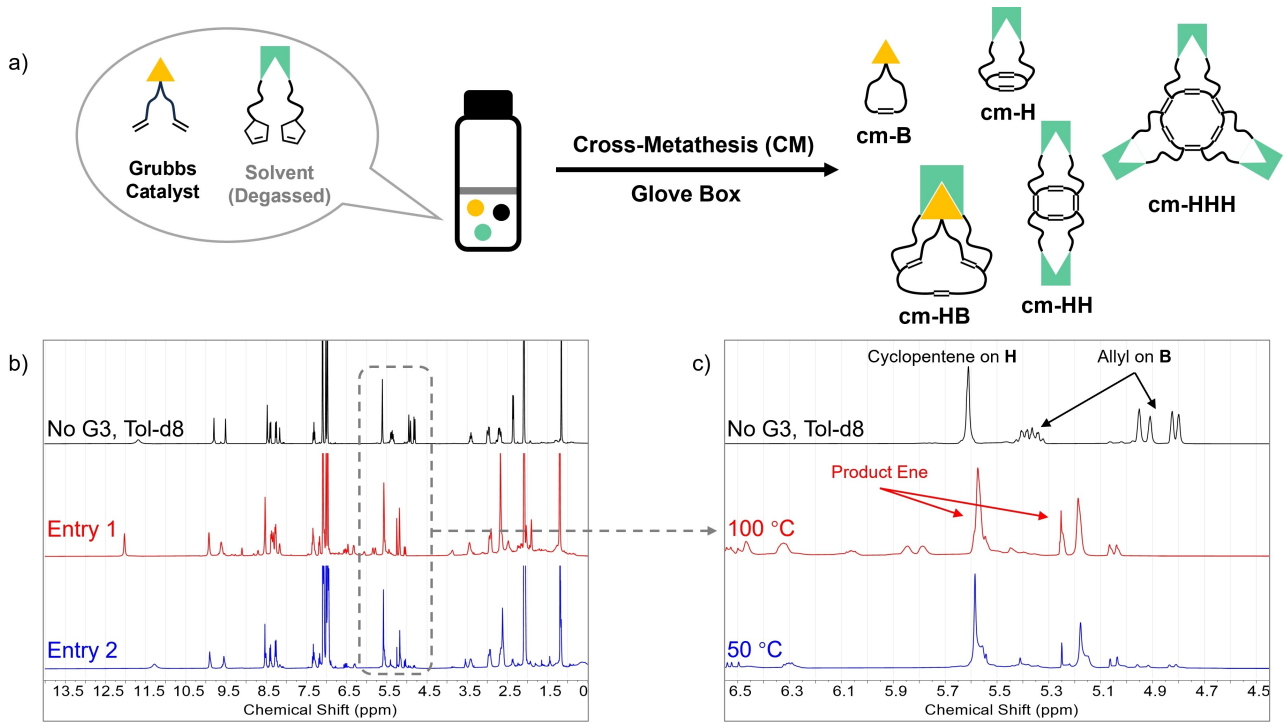

Figure 4. a) Schematic explanation to conduct cross-metathesis (**CM**) reactions to fix the **H**–**B** model complexes; forming oligomers (representative structures cm (B, H, HB, HH, HHH) are shown) b) ^{1}H NMR spectrum of the reaction mixture from Entry 1 and 2, see Table 3; The zoom-in of the double bond region of the ^{1}H NMR spectrum.

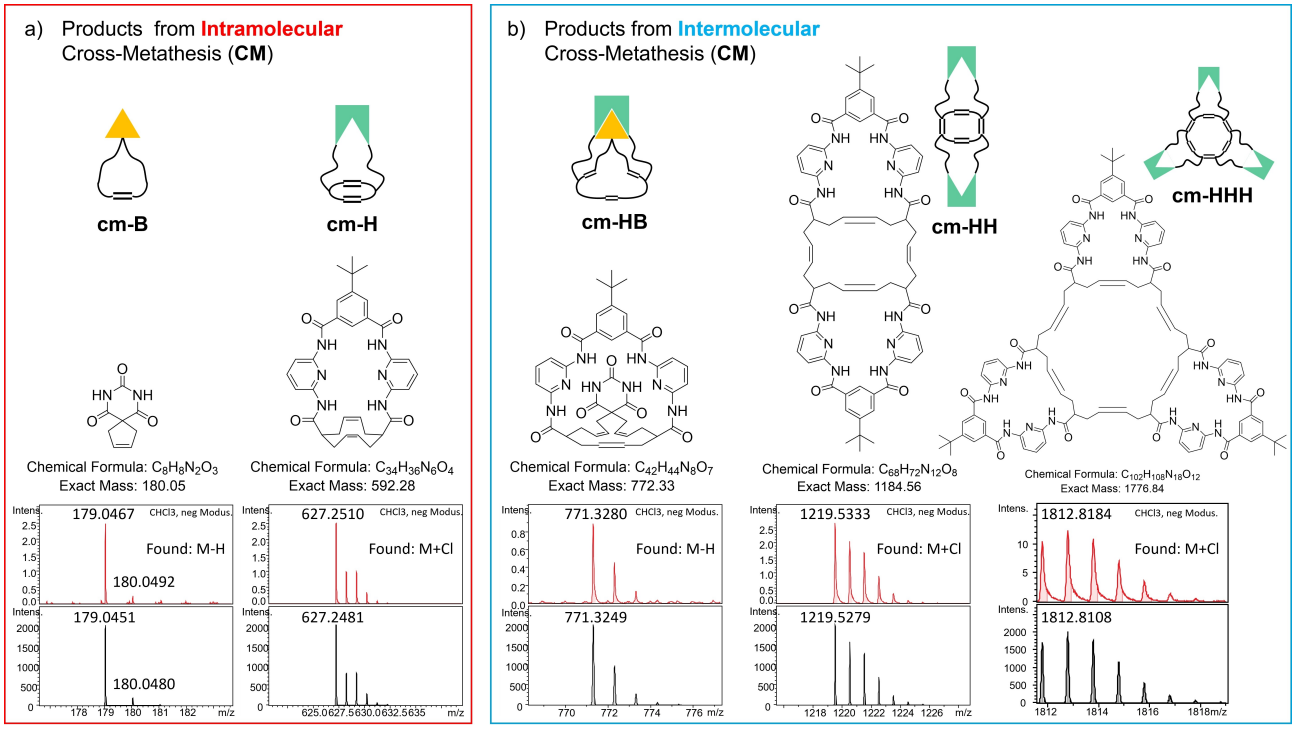

Figure 5. Representative products from Entry 1 (experimental condition: Tol-d_8, **H** or **B** in a 1 : 1 ratio at 0.01 M, G3 catalyst) found by ESI MS using negative modus without salt (for simulation of all ions, constitutional isomers, and intermediates from cross-metathesis reactions for all entries, see the attached *Supporting Information*, SI 3 and SI PDF file: ESI Analysis_All Entries).

cyclopentene moieties in a single molecule. As depicted in Figure 5b), the model host–guest complex fixed by the **CM** reaction was found as **cm-HB**. Although the temperature was kept to 100 °C, a pretty harsh condition to maintain the host–

guest complex, **cm-HB**, **cm-HH**, and **cm-HHH** complexes were identified, with the dimers (**cm-HH**) and trimers (**cm-HHH**) being present, beyond our expectation, which were identified by the ESI MS analysis (the constitutional isomers of **cm-HH** and **cm-HHH** can be found in *Supporting Information*, SI 3). These oligomers can be attributed to the self-association of **H** and the potentially higher reactivity of the cyclopentene moieties compared to the allyl groups on **B**. Probing different reaction conditions (see Table 3), we could identify all those products with different temperatures and concentrations (as possible and partially limited by the reduced solubility of **H** and **B** under specific conditions). Nevertheless, the intermediate product bearing a styrene residue from the Grubbs catalyst was found for all entries, together demonstrating the successful **CM** reactions affording the similarly fixed individual model compounds and their possible aggregates (for the analysis of all products and intermediates for all entries, see *Supporting Information*, SI 3, and the attached PDF file: ESI Analysis_All Entries).

We then went one step further to reveal the relative ratios of the different ions of the different host–guest complexes since ESI MS not only can qualitatively identify the products[30] but also allows us to semi-quantitatively extract the relative ratios among the **CM** products, which are essential to further study changes in response to different reaction conditions (concentration, solvent, temperature). In line with previous work on protein/lipid complexes,[31] we used the intensity of individual peaks representing a specific product to calculate the normalized product percentage within one measurement, provided that all **CM** products have similar structures and should demonstrate equal ionization in the ESI process. As there are multiple ions for one **CM** product, the intensity of all the relevant ion couplings for this respective product was summed as cumulative intensity and used for calculation (for calculation details, see *Supporting Information*, SI 3).

Indeed, the fixed H-bond-mediated products demonstrate different normalized product ratios due to the applied conditions influencing the H-bonds. The calculation and the analysis results for all entries are summarized in Table 4, with the schematic formulas provided therein, focusing on the major products detected and identified via ESI MS. In Entry 1–6, the **CM** product of **cm-B** is present in only a negligible percentage. This low percentage of **cm-B** could result from the low reactivity of the allyl group to form the target cyclopentene ring, impeding the ring-closing **CM** reactions catalyzed by the Grubbs catalyst. By contrast, due to the relatively low concentration applied and the high reactivity of cyclopentene moieties driven by the ring strain, the cyclic product **cm-H** shows the highest ratio among all products, ranging from 74.47% (Entry 4) to 95.22% (Entry 5). As the temperature was decreased from 100 °C (Entry 1) to 50 °C (Entry 2), expected to promote the formation of the **H**–**B** host–guest complex via the intermolecular H-bonds, the amount of **cm-H** shows a decreasing ratio from 91.89% to 75.96%, with a concomitant increase of the fixed complex **cm-HB** from 1.62% to 4.62%. When concentration increased from 0.01 M (Entry 2) to 0.1 M (Entry 3), the formation of the **H**–**B** complex should be favored, visible by the now changed product (**cm-HB**) ratio (4.62% vs. 9.07%), in line with expectations.

The experimental conditions (solvents, temperature) strongly influence the aggregation/association of the formed **CM** products. In Figure 6, the ratio of the fixed aggregated products, namely **cm-HB**, **cm-HH** for the dimer, and **cm-HHH** for the trimer, were plotted to illustrate the obtained product ratios. For Entry 1, using 100 °C in Tol-d_8 to fix the aggregates with a quantitative conversion, most H-bonds accounting for the formation of the host–guest complexes were also destroyed, showing the product **cm-HB** as a consequence with the lowest percentage of 1.63%, comparable to that in Entry 4 where the H-bond-replacing solvent MeOD was used though at 50 °C. These two comparable amounts of the **H**–**B** host–guest

Table 4. Normalized product percentages calculated based on ESI MS intensities of each product.

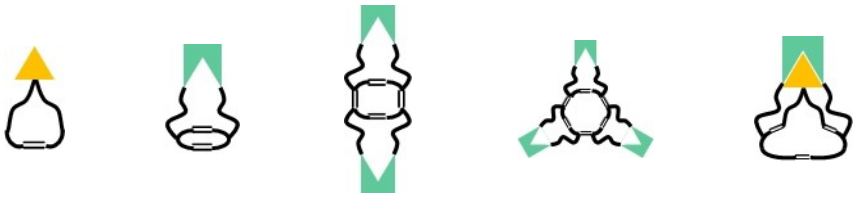

Entry [a]	Experimental Conditions	cm-B	cm-H	cm-HH [b]	cm-HHH [b]	cm-HB
1	Tol-d_8_100 °C_0.01 M	0.24%	91.89%	5.93%	0.23%	1.63%
2	Tol-d_8_50 °C_0.01 M	0.31%	75.96%	12.81%	6.30%	4.62%
3	DCE_50 °C_0.1 M	–	87.98%	2.55%	0.40%	9.07%
4	MeOD_50 °C_0.01 M	0.08%	74.47%	15.25%	8.35%	1.84%
5	DCE_50 °C_0.1 M_G2	–	95.22%	2.16%	0.32%	2.30%
6	PIB_50 °C	1.67%	81.12%	7.01%	2.92%	7.28%

* [a] The normalized percentages were calculated based on the cumulative intensity of the products in ESI MS spectra; for detailed calculation, see *Supporting Information*, SI 3; [b] the structures of **cm-HH** and **cm-HHH** here were selected as representatives, and their constitutional isomers can be found in the *Supporting Information*, SI 3.

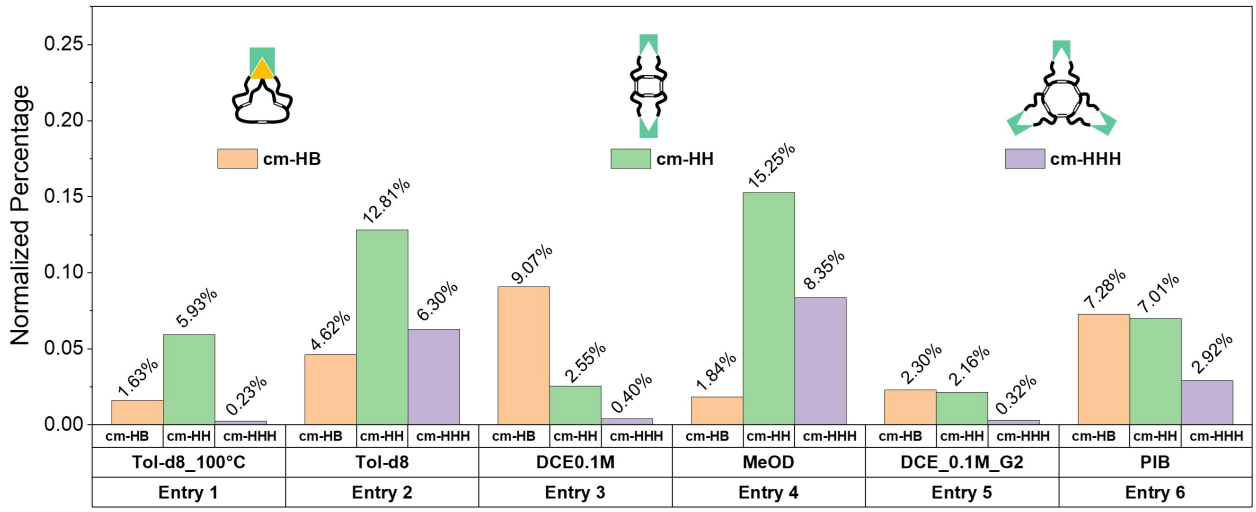

Figure 6. Normalized percentage of selected products for Entry 1–6 (the normalized percentage was calculated based on the cumulative intensity of the products in ESI MS spectra; for detailed calculation, see *Supporting Information*, SI 3; the structures of **cm-HH** and **cm-HHH** here were selected as representatives, and their constitutional isomers can be found in *Supporting Information*, SI 3.)

complex in Tol at 100 °C and in MeOH at 50 °C reveal that elevation of temperature weakens the H-bonds and the resulting host–guest complex in a similar manner as the change of the solvent from an H-bond-maintaining Tol-d_8 to an H-bond-replacing MeOD. When the temperature was reduced to 50 °C (Entry 2), the percentage of the dimeric aggregate, **cm-HH**, increased to 4.62 %, as expected. Increasing the concentration of the reactants **H** and **B** to 0.1 M (Entry 3) led to an increase in the specific **H**–**B** host–guest complex, yielding **cm-HB** with the highest percentage of 9.07 % among all the products. Owing to the promoted reactivity of cyclopentene moieties on **H** in **CM** reaction compared to allyl groups on **B**, in Entry 1, 2, and 4, the aggregated **cm-HH** and **cm-HHH** demonstrate higher percentages than the associated **cm-HB**. However, this ratio is lower than **cm-HB** if the solvent is replaced by DCE (Entry 3 and 5). For Entry 4, though MeOH was added to the reaction medium, **cm-HH** and **cm-HHH** are formed in high percentages, which we attribute to the closer proximity among the aromatic rings driven by hydrophobic interaction from pi-pi stacking over the now strongly diminished H-bonds as destroyed by the polar protic nature of MeOH.

Cross-Metathesis (CM) Reaction in a Solvent-Free Polymeric Environment - inside a Polyisobutylene (PIB) Matrix

As described in Table 3 and Table 4, Entry 6 **CM** was conducted to fix the **H**–**B** model host–guest complex and the possible aggregates inside a **PIB** matrix and further subject to the ESI MS analysis. As illustrated in Figure 7a), the **H** and **B** model compounds, the G3 catalyst, and the **PIB** matrix (M_n = 1300 Da) were placed in a vial, and degassed THF was added. After all components were dissolved, THF was removed at room temperature using a rotary evaporator, followed by an ultra-high vacuum to remove all THF residue. After refilling with argon, the vial was heated at 50 °C in a glovebox to promote the **CM** reaction. After 24 hours, the reaction was removed from the glovebox and diluted with a minimum amount of THF, followed by digestion in *n*-hexane and MeOH to separate the **PIB** matrix from the formed **CM** products in a separation funnel. After recovery from the MeOH phase, the herein soluble products (devoid of the **PIB** matrix, which was selectively removed by the *n*-hexane) were analyzed firstly via ^{1}H NMR spectroscopy to prove conversion (see Figures 7b&c). As the **CM** reaction was conducted without a solvent, different ratios of the host–guest complexes were expected to form. The chemical shifts of the alkene moieties at δ = 5.65 and 5.20 ppm of **B** vanished almost completely, and a new singlet peak at δ = 5.65 ppm was formed, indicative of a successful **CM** reaction. In addition, the starting resonances **H** at δ = 5.74 ppm vanished, with a new resonance appearing at δ = 5.72 ppm, demonstrating the conversion of the model compounds (97.3 %, see Table 3, Entry 6). Further, the fixed complexes/aggregates were analyzed by the method developed previously using ESI MS. As depicted in Figure 6, the fixed host–guest **cm-HB** demonstrates a product ratio of 7.28 %, comparable to that in Entry 3 using a 0.1 M model compound concentration. The fixed dimer **cm-HH** was found with a product ratio of 7.01 % for the aggregated products. In comparison, the fixed trimer **cm-HHH** demonstrated the highest ratio of 2.92 % among all entries due to the promoted aggregation by the nonpolar and non-H-bond-replacing **PIB** bulk.

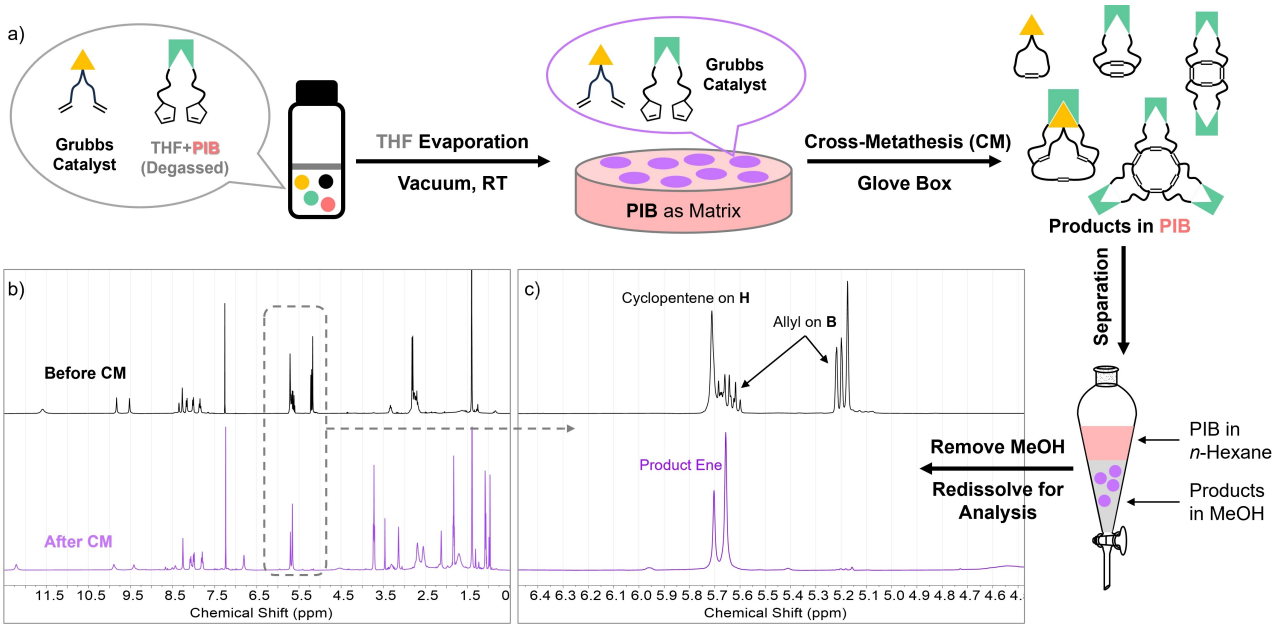

Figure 7. a) Schematic explanation of cross-metathesis (**CM**) reaction in a polyisobutylene (**PIB**) matrix and the workup to remove **PIB** matrix; b) ^{1}H NMR (in $CDCl_3$) of the products mixture before the addition of catalyst and after workup to remove **PIB** matrix; c) zoom-in of the double bond region of the ^{1}H NMR spectrum; the vanish of the starting alkene shifts indicates the high conversion (97.3 %) of Entry 6 (see Table 3).

We further probed diffusion-ordered NMR spectroscopy (DOSY) to distinguish the different products based on their diffusion coefficients, similar to the reported identification of complex mixtures without separation.[32] After the workup, as described in Entry 6, the product mixture was directly probed. As shown in Figure 8, the newly formed alkene resonance at $\delta = 5.65$ ppm and the peak at $\delta = 5.72$ ppm can be clearly distinguished on the DOSY spectrum. Indicated by the yellow arrows, the resonances at $\delta = 5.72$&3.25 and $\delta = 1.0$–1.5 ppm illustrate the **CM** products of barbiturate **cm-B** and the aggregated oligomers with a diffusion coefficient of 6.50×10^{-5} cm^2 s^{-1}. The alkene resonances at $\delta = 5.68$ ppm (see green arrows), together with the phenyl-resonances (Ph–) at $\delta = 7.5$–8.5 ppm, demonstrate a reduced diffusion coefficient of 5.50×10^{-5} cm^2 s^{-1}, which can be assigned to the fixed host–guest complex **cm-HB** as well as the aggregated products **cm-HH** and **cm-HHH**. Thus, with the assistance of DOSY, various products can be further identified without separation. When our method for aggregate analysis is applied to study H-bonded aggregates in polymers, the resulting **CM** products with polymeric backbones can be distinguished by DOSY, hence facilitating the MS analysis which is typically more challenging when dealing with polymers.

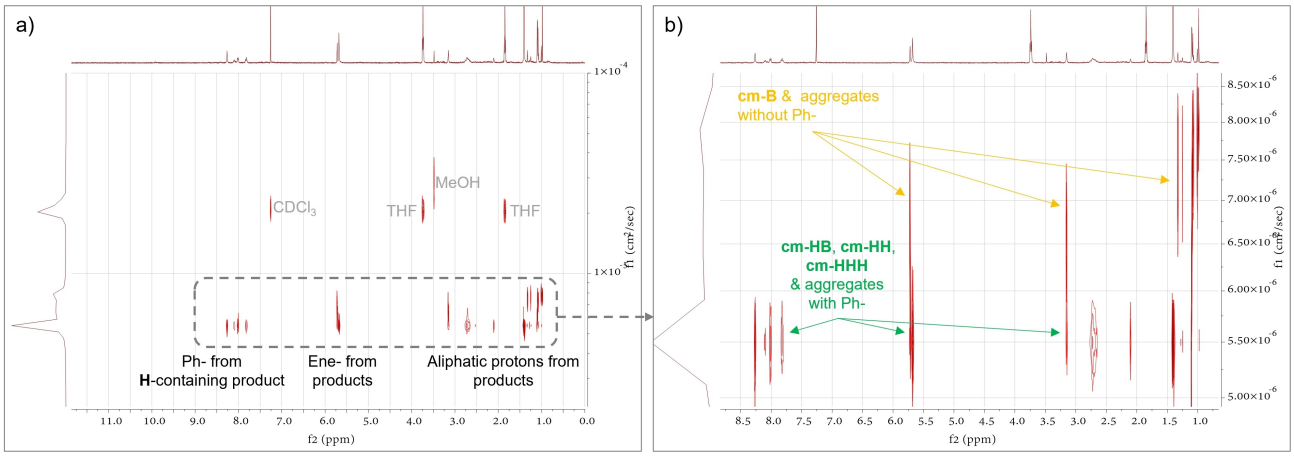

Figure 8. a) Diffusion-ordered NMR spectroscopy (DOSY) spectrum of the products mixture from Entry 6 directly after workup; b) the zoom-in of the region of product signals. (the alkene and other shifts referred by the yellow arrows are attributed to the fixed products of **cm-B** and possible aggregates as evidenced by a lack of phenyl (Ph–) shifts, while the alkene and other shifts referred by the green arrows are attributed to the fixed products **cm-HB**, as well as the aggregated products **cm-HH** and **cm-HHH**).

Conclusions

We here experimentally probed the formation of host–guest complexes of Hamilton receptor-barbiturate (**H**–**B**) complexes, formed in solution and inside a polymer matrix, to probe the influence of a microenvironment on their supramolecular association behavior. A new method was developed to firstly covalently fix the H-bonded associates/aggregates via an alkene cross-metathesis (**CM**) reaction, followed by analysis of these then covalently linked aggregates using electrospray ionization mass spectrometry (ESI MS). To this end, a novel Hamilton receptor (**H**) was equipped with cyclopentene moieties and used as a host to form host–guest complexes with allobarbital (**B**), as studied via UV-Vis spectroscopy titration experiments in different solvents and at various temperatures. These experiments allowed us to validate the formation of the specific host–guest complexes. Furthermore, it is observed that polar solvents containing additional H-bonding sites significantly reduce the formation of the 1:1 **H**–**B** complex, indicated by an association constant of **H**–**B**, weakened from $K_{assn.} = \sim 10^5\ M^{-1}$ in toluene, to $\sim 10^4\ M^{-1}$ in halogenated solvents (chloroform, DCM), further to $\sim 10^3\ M^{-1}$ in 1,2-dichloroethane, and finally, to $\sim 10^2\ M^{-1}$ in polar H-bonding-replacing solvents such as MeOH, HFiP, and DMSO. In addition, the presence of 0.2 equivalents of methanol in toluene significantly reduced $K_{assn.}$ to $\sim 10^2\ M^{-1}$, comparable to other polar H-bonding-replacing solvents. To probe the cross-metathesis (**CM**) chemistry for covalent fixation of the H-bonded structures, we probed Grubbs 2nd and Grubbs 3rd generation catalysts under several reaction conditions (solvent, temperature, and concentration), identifying the optimal reaction conditions at 50 °C. Higher-order aggregates (dimers **cm-HH** and trimers **cm-HHH**, denoted after **CM** reactions) were covalently tethered via **CM** reaction, followed by electrospray ionization mass spectrometry (ESI MS) analysis. This two-step method, first a covalent **CM** fixation followed by ESI MS, was extended to study the **H**–**B** model complex within a polyisobutylene (**PIB**) matrix, presenting a method to analyze the complex host–guest assemblies in solvent-free (polymeric) environments. The results indicated a higher percentage of H-bonded 1:1 **H**–**B** assembly, **cm-HB**, and an increased amount of dimers, **cm-HH**, and trimers, **cm-HHH**, due to the closer proximity among the model compounds and the related segregation effects from the surrounding polymer matrix. This approach successfully established a two-step method to study H-bonded assemblies, allowing to be identified via ESI MS analysis, even inside concentrated or solvent-free systems, such as in a model polymer (polyisobutylene, **PIB**). This approach, therefore, opens a new perspective to reveal the formation of aggregates and complex assemblies, potentially avoiding the need for laborious physical characterizations such as SAXS/WAXS.

Acknowledgements

The authors are grateful to the DFG project INST 271/444-1 FUGG for financial support; the DFG-Project BI1337/18-1, BI1337/17-1, DFG-Project BI1337/16-1; BI1337/14-1 and the GRK 2670, W69000789, Project Nr 436494874. Open Access funding enabled and organized by Projekt DEAL.

Conflict of Interests

The authors declare no conflict of interest.

Data Availability Statement

The data that support the findings of this study are available in the supplementary material of this article.

Keywords: Aggregates · Association constants · Barbiturate · Hamilton receptor · Hydrogen bonds

[1] a) T. Aida, E. W. Meijer, S. I. Stupp, *Science* **2012**, *335*, 813–817; b) S. Chen, T. Yan, M. Fischer, A. Mordvinkin, K. Saalwächter, T. Thurn-Albrecht, W. H. Binder, *Angew. Chem. Int. Ed.* **2017**, *56*, 13016–13020; c) S. Chen, W. H. Binder, *Acc. Chem. Res.* **2016**, *49*, 1409–1420; d) S. V. Wanasinghe, E. M. Schreiber, A. M. Thompson, J. L. Sparks, D. Konkolewicz, *Polym. Chem.* **2021**, *12*, 1975–1982.
[2] A. J. Greenlee, C. I. Wendell, M. M. Cencer, S. D. Laffoon, J. S. Moore, *Trends Chem.* **2020**, *2*, 1043–1051.
[3] a) C. Li, R. Bhandary, A. Marinow, D. Ivanov, M. Du, R. Androsch, W. H. Binder, *Polymers (Basel)* **2022**, *14*, 4090; b) S. Chen, Z. Li, Y. Wu, N. Mahmood, F. Lortie, J. Bernard, W. H. Binder, J. Zhu, *Angew. Chem. Int. Ed.* **2022**, *61*, e202203876; c) C. Li, P. Hilgeroth, N. Hasan, D. Ströhl, J. Kressler, W. H. Binder, *Int. J. Mol. Sci.* **2021**, *22*, 12679.
[4] J. Sartorius, H.-J. Schneider, *Chem. Eur. J.* **1996**, *2*, 1446–1452.
[5] S. Chen, N. Mahmood, M. Beiner, W. H. Binder, *Angew. Chem., Int. Ed.* **2015**, *54*, 10188–10192.
[6] a) T. Yan, K. Schröter, F. Herbst, W. H. Binder, T. Thurn-Albrecht, *Macromolecules* **2017**, *50*, 2973–2985; b) X. Callies, C. Vechambre, C. Fonteneau, F. Herbst, J. M. Chenal, S. Pensec, L. Chazeau, W. H. Binder, L. Bouteiller, C. Creton, *Soft Matter.* **2017**, *13*, 7979–7990; c) T. Yan, K. Schröter, F. Herbst, W. H. Binder, T. Thurn-Albrecht, *Macromolecules* **2014**, *47*, 2122–2130; d) F. Herbst, W. H. Binder, *Polym. Chem.* **2013**, *4*, 3602–3609.
[7] a) F. Herbst, W. H. Binder, *Polym. Chem.* **2013**, *4*, 3602–3609; b) S. H. M. Söntjens, R. P. Sijbesma, M. H. P. van Genderen, E. W. Meijer, *J. Am. Chem. Soc.* **2000**, *122*, 7487–7493.
[8] A. Mordvinkin, D. Döhler, W. H. Binder, R. H. Colby, K. Saalwächter, *Phys. Rev. Lett.* **2020**, *125*, 127801.
[9] W. H. Binder, S. Bernstorff, C. Kluger, L. Petraru, M. J. Kunz, *Adv. Mater.* **2005**, *17*, 2824–2828.
[10] S. Valkama, T. Ruotsalainen, A. Nykänen, A. Laiho, H. Kosonen, G. ten Brinke, O. Ikkala, J. Ruokolainen, *Macromolecules* **2006**, *39*, 9327–9336.
[11] a) F. Herbst, K. Schröter, I. Gunkel, S. Gröger, T. Thurn-Albrecht, J. Balbach, W. H. Binder, *Macromolecules* **2010**, *43*, 10006–10016; b) M. Ahmadi, A. Jangizehi, S. Seiffert, *Macromolecules* **2022**, *55*, 5514–5526; c) X. Huang, S. Nakagawa, H. Houjou, N. Yoshie, *Macromolecules* **2021**, *54*, 4070–4080; d) M. Golkaram, K. Loos, *Macromolecules* **2019**, *52*, 9427–9444; e) A. Shabbir, H. Goldansaz, O. Hassager, E. van Ruymbeke, N. J. Alvarez, *Macromolecules* **2015**, *48*, 5988–5996; f) C. L. Lewis, K. Stewart, M. Anthamatten, *Macromolecules* **2014**, *47*, 729–740; g) K. E. Feldman, M. J. Kade, E. W. Meijer, C. J. Hawker, E. J. Kramer, *Macromolecules* **2009**, *42*, 9072–9081; h) T. Yan, K. Schröter, F. Herbst, W. H. Binder, T. Thurn-Albrecht, *Sci. Rep* **2016**, *6*, 32356; i) S. Chen, D. Döhler, W. H. Binder, *Polymer* **2016**, *107*, 466–473.
[12] a) R. Zhang, W. Chen, T. Miyoshi, *Macromolecules* **2024**, *57*, 1893–1918; b) F. Wang, P. Sun, *Acta Polym. Sin.* **2021**, *52*, 840–856; c) A. Mordvinkin, D. Döhler, W. H. Binder, R. H. Colby, K. Saalwächter, *Phys. Rev. Lett.* **2020**, *125*; d) B. Fortier-McGill, V. Toader, L. Reven, *Macromolecules* **2012**, *45*, 6015–6026; e) B. Li, L. Xu, Q. Wu, T. Chen, P. Sun, Q. Jin, D. Ding, X.

Wang, G. Xue, A.-C. Shi, *Macromolecules* **2007**, *40*, 5776–5786; f) C. Li, R. Bhandary, A. Marinow, S. Bachmann, A.-C. Pöppler, W. H. Binder, *Macromol. Rapid Commun.* **2023**, *45*, 2300464.
[13] a) A. Mordvinkin, D. Döhler, W. H. Binder, R. H. Colby, K. Saalwächter, *Macromolecules* **2021**, *54*, 5065–5076; b) A. R. Brás, C. H. Hövelmann, W. Antonius, J. Teixeira, A. Radulescu, J. Allgaier, W. Pyckhout-Hintzen, A. Wischnewski, D. Richter, *Macromolecules* **2013**, *46*, 9446–9454; c) E. Ostas, T. Yan, T. Thurn-Albrecht, W. H. Binder, *Macromolecules* **2013**, *46*, 4481–4490; d) S. Chen, Y. Wu, H. Wang, B. Zhu, B. Xiong, W. H. Binder, J. Zhu, *Polym. Chem.* **2021**, *12*, 4111–4119; e) B. N. Narasimhan, A. W. Dixon, B. Mansel, A. Taberner, J. Mata, J. Malmström, *J. Colloid Interface Sci.* **2023**, *630*, 638–653; f) S. Lettieri, P. Manesiotis, M. Slann, D. W. Lewis, A. J. Hall, *React. Funct. Polym.* **2021**, *167*, 105031.
[14] S. Chen, W. H. Binder, *Acc. Chem. Res.* **2016**, *49*, 1409–1420.
[15] S. K. Chang, A. D. Hamilton, *J. Am. Chem. Soc.* **1988**, *110*, 1318–1319.
[16] a) D. T. Seidenkranz, M. D. Pluth, *J. Org. Chem.* **2019**, *84*, 8571–8577; b) D. T. Seidenkranz, J. M. McGrath, L. N. Zakharov, M. D. Pluth, *Chem. Commun.* **2017**, *53*, 561–564; c) J. M. McGrath, M. D. Pluth, *J. Org. Chem.* **2014**, *79*, 711–719; d) Y. Molard, D. M. Bassani, J.-P. Desvergne, P. N. Horton, M. B. Hursthouse, J. H. R. Tucker, *Angew. Chem. Int. Ed.* **2005**, *44*, 1072–1075; e) S. R. Collinson, J. H. R. Tucker, T. Gelbrich, M. B. Hursthouse, *Chem. Commun.* **2001**, 555–556; f) J. Westwood, S. J. Coles, S. R. Collinson, G. Gasser, S. J. Green, M. B. Hursthouse, M. E. Light, J. H. R. Tucker, *Organometallics* **2004**, *23*, 946–951.
[17] a) J. J. Du, J. R. Hanrahan, V. R. Solomon, P. A. Williams, P. W. Groundwater, J. Overgaard, J. A. Platts, D. E. Hibbs, *J. Phys. Chem. A* **2018**, *122*, 3031–3044; b) T. Ema, K. Hamada, K. Sugita, Y. Nagata, T. Sakai, A. Ohnishi, *J. Org. Chem.* **2010**, *75*, 4492–4500; c) A. Tron, P. J. Thornton, B. Kauffmann, J. H. R. Tucker, N. D. McClenaghan, *Supramol. Chem.* **2016**, *28*, 733–741; d) S. Lakkakula, O. D. Mitkin, R. A. Valiulin, A. G. Kutateladze, *Org. Lett.* **2007**, *9*, 1077–1079; e) H. S. Sørensen, J. Larsen, B. S. Rasmussen, B. Laursen, S. G. Hansen, T. Skrydstrup, C. Amatore, A. Jutand, *Organometallics* **2002**, *21*, 5243–5253; f) M. H. Al-Sayah, R. McDonald, N. R. Branda, *Eur. J. Org. Chem.* **2004**, *2004*, 173–182.
[18] O. A. Scherman, G. B. W. L. Ligthart, H. Ohkawa, R. P. Sijbesma, E. W. Meijer, *Proc. Natl. Acad. Sci.* **2006**, *103*, 11850–11855.
[19] a) A. D. Hamilton, A. Muehldorf, S.-K. Chang, N. Pant, S. Goswami, D. van Engen, *J. Inclusion Phenom. Mol. Recognit. Chem.* **1989**, *7*, 27–38; b) S. K. Chang, D. Van Engen, E. Fan, A. D. Hamilton, *J. Am. Chem. Soc.* **1991**, *113*, 7640–7645.
[20] a) K. Hager, U. Hartnagel, A. Hirsch, *Eur. J. Org. Chem.* **2007**, *2007*, 1942–1956; b) T. Ema, D. Tanida, K. Sugita, T. Sakai, K.-i. Miyazawa, A. Ohnishi, *Org. Lett.* **2008**, *10*, 2365–2368; c) M. Ali, E. Kataev, J. Müller, H. Park, M. Halik, A. Hirsch, *Chem. - Eur. J.* **2021**, *27*, 16429–16439; d) N. M.-W. Wu, V. W.-W. Yam, *ACS Appl. Mater. Interfaces* **2019**, *11*, 40290–40299; e) F. Wessendorf, B. Grimm, D. M. Guldi, A. Hirsch, *J. Am. Chem. Soc.* **2010**, *132*, 10786–10795; f) F. Wessendorf, A. Hirsch, *Tetrahedron* **2008**, *64*, 11480–11489.
[21] a) A. Croom, K. B. Manning, M. Weck, *Macromolecules* **2016**, *49*, 7117–7128; b) R. Schmidt, M. Stolte, M. Grüne, F. Würthner, *Macromolecules* **2011**, *44*, 3766–3776.
[22] S. Chen, B.-D. Lechner, A. Meister, W. H. Binder, *Nano Lett.* **2016**, *16*, 1491–1496.
[23] I. M. Smallwood, *Handbook of Organic Solvent Properties*, Arnold, a member of the Hodder Headline Group, 338 Euston Road, London NW1 3BH, Great Britain, **1996**.
[24] P. Thordarson, *Chem. Soc. Rev.* **2011**, *40*, 1305–1323.
[25] D. Brynn Hibbert, P. Thordarson, *Chem. Commun.* **2016**, *52*, 12792–12805.
[26] a) C. A. Hunter, *Angew. Chem. Int. Ed.* **2004**, *43*, 5310–5324; b) J. L. Cook, C. A. Hunter, C. M. R. Low, A. Perez-Velasco, J. G. Vinter, *Angew. Chem. Int. Ed.* **2007**, *46*, 3706–3709.
[27] a) S. Alavi, R. Susilo, J. A. Ripmeester, *J Chem Phys* **2009**, *130*, 174501; b) L. Wen, J. Zhang, T. Zhou, A. Zhang, *Vib. Spectrosc.* **2016**, *86*, 160–172; c) W. Suzuki, H. Kotani, T. Ishizuka, K. Ohkubo, Y. Shiota, K. Yoshizawa, S. Fukuzumi, T. Kojima, *Chem. - Eur. J.* **2017**, *23*, 4669–4679.
[28] S.-I. Kondo, T. Hayashi, Y. Sakuno, Y. Takezawa, T. Yokoyama, M. Unno, Y. Yano, *Org. Biomol. Chem.* **2007**, *5*, 907.
[29] a) T. Galaon, V. David, *J. Sep. Sci.* **2011**, *34*, 1423–1428; b) K. Ueda, K. Higashi, K. Moribe, L. S. Taylor, *Mol. Pharmaceutics* **2022**, *19*, 100–114.
[30] a) H. Wang, S. Hanash, *Humana Press* **2009**, 227–242; b) D. T. Bui, Z. Li, P. I. Kitov, L. Han, E. N. Kitova, M. Fortier, C. Fuselier, P. Granger Joly de Boissel, D. Chatenet, N. Doucet, S. M. Tompkins, Y. St-Pierre, L. K. Mahal, J. S. Klassen, *ACS Cent. Sci.* **2022**, *8*, 963–974.
[31] a) T. Kundlacz, C. Schmidt, *Anal. Chem.* **2023**, *95*, 17292–17299; b) W. Lu, X. Yin, X. Liu, G. Yan, P. Yang, *Sci. China: Chem.* **2014**, *57*, 686–694; c) S. Pérez-Rafael, S. Atrian, M. Capdevila, Ò. Palacios, *Talanta* **2011**, *83*, 1057–1061.
[32] a) P. Groves, *Polym. Chem.* **2017**, *8*, 6700–6708; b) E. F. Dudás, A. Bodor, *Anal. Chem.* **2019**, *91*, 4929–4933; c) E. Ruzicka, P. Pellechia, B. C. Benicewicz, *Anal. Chem.* **2023**, *95*, 7849–7854.
[33] a) P. C. Srivastava, A. P. Callahan, E. B. Cunningham, F. F. Knapp, Jr., *J. Med. Chem.* **1983**, *26*, 742–746; b) Mohammad, R. McDonald, Neil, *Eur. J. Org. Chem.* **2004**, *2004*, 173–182; c) H. Rupp, D. Döhler, P. Hilgeroth, N. Mahmood, M. Beiner, W. H. Binder, *Macromol. Rapid Commun.* **2019**, *40*, 1900467; d) R. Appel, *Angew. Chem., Int. Ed. Engl.* **1975**, *14*, 801–811.

Manuscript received: October 24, 2024
Accepted manuscript online: November 12, 2024
Version of record online: November 21, 2024